DSP-based Robust Nonlinear Speed Control of PM Synchronous Motor Using Adaptive and Sliding Mode Control Techniques

In-Cheol Baik, Kyeong-Hwa Kim, Kwan-Yuhl Cho, and Myung-Joong Youn

Abstract

A DSP-based robust nonlinear speed control of a permanent magnet synchronous motor(PMSM) which is robust to unknown parameter variations and speed measurement error is presented. The model reference adaptive system(MRAS) based adaptation mechanisms for the estimation of slowly varying parameters are derived using the Lyapunov stability theory. For the disturbances or quickly varying parameters, a quasi-linearized and decoupled model including the influence of parameter variations and speed measurement error on the nonlinear speed control of a PMSM is derived. Based on this model, a boundary layer integral sliding mode controller to improve the robustness and performance of the nonlinear speed control of a PMSM is designed and compared with the conventional controller. To show the validity of the proposed control scheme, simulations and experimental works are carried out and compared with the conventional control scheme.

I. Introduction

PMSM drives are being increasingly used in a wide range of applications due to their high power density, large torque to inertia ratio, and high efficiency. This paper deals with the nonlinear speed control of a surface mounted permanent magnet synchronous motor with sinusoidal flux distribution. Since the dynamics of the currents is much faster than that of the mechanical speed, the speed is considered as a constant parameter rather than a state variable and they can be approximately linearized by the field orientation and current control [1-4]. However, for low power servo drives, this approximate linearization leads to the lack of torque due to the incomplete current control during the speed transient and reduces the control performance [5-6].

A solution to overcome this problem proposed by Le Pioufle [7] is to consider the motor speed as a state variable in electrical equations, which results in a nonlinear model. Then the nonlinear control method, so called feedback linearization technique, is applied to obtain an exactly linearized and decoupled model and the linear design technique is employed to complete the control design [8]. Since the nonlinear controller is very sensitive to the speed measurement error, even small error of speed measurement results in a significant speed error and its robustness can be improved by carefully selecting the control gains in the linear control loops [7]. However, besides the speed measurement error, there are parameter variations such as the stator resistance, flux, and inertia due to the temperature rise and load variations. The stator resistance and flux variations also show a steady state error and the inertia and flux variations degrade transient performance. The steady state error may also go to zero by properly choosing the linear controller gains. However, the transient performance can still be significantly degraded due to the inertia and flux variations.

The feedback linearization deals with the technique of transforming the original system model into an equivalent model of a simpler form, and then employs the well-known and powerful linear design technique to complete the control design. However, it does not guarantee the robustness in the presence of parameter uncertainties or disturbances and the drawbacks of the conventional nonlinear control scheme result from this fact.

To overcome these drawbacks, various control techniques such as adaptive control and sliding mode control can be considered. Generally, an adaptive control technique is superior to a sliding mode control in dealing with

Manuscript received December 26, 1997; accepted February 11, 1998.
The authors are with the Department of Electrical Engineering, Korea Advanced Institute of Science and Technology.

uncertainties of constant or slowly varying parameters. Conversely, a sliding mode control has some desirable features, such as its ability to deal with disturbances or quickly varying parameters [9]. Among the above mentioned parameters and disturbances, the resistance and flux are slowly varying parameters because their variations are mainly due to the temperature rises. On the contrary, the inertia can not be easily estimated using the adaptive technique because the load inertia can be abruptly and frequently changed due to the payload changes, etc., and its influence is only for a short transient period.

Therefore, in this paper, the MRAS-based adaptation mechanisms for the estimation of slowly varying parameters are derived using the Lyapunov stability theory. For the disturbances and quickly varying parameters, the feedback linearization technique is considered as a model-simplifying device for the robust control [9]. For this purpose, a quasi-linearized and decoupled model including the influence of parameter variations and speed measurement error on the nonlinear speed control of a PMSM is first derived and then the robust control scheme employing a boundary layer integral sliding mode is designed to improve the control performance.

II. Nonlinear Speed Control of PMSM using Input-Output Linearization

1. Modeling of PMSM

The machine considered is a surface mounted PMSM and the nonlinear state equation in the synchronous dq reference frame can be represented as follows :

$$\frac{dx}{dt} = f(x) + Gu \tag{1}$$

where

$$x = \begin{pmatrix} x_1 \\ x_2 \\ x_3 \end{pmatrix} = \begin{pmatrix} i_d \\ i_q \\ \Omega \end{pmatrix} \tag{2}$$

$$u = \begin{pmatrix} u_1 \\ u_2 \end{pmatrix} = \begin{pmatrix} v_d \\ v_q \end{pmatrix} \tag{3}$$

$$G = \begin{pmatrix} \frac{1}{L_d} & 0 \\ 0 & \frac{1}{L_q} \\ 0 & 0 \end{pmatrix} \tag{4}$$

$$f(x) = \begin{pmatrix} f_1(x) \\ f_2(x) \\ f_3(x) \end{pmatrix} = \begin{pmatrix} -\frac{R}{L_d} x_1 + P\frac{L_q}{L_d} x_2 x_3 \\ -P\frac{L_d}{L_q} x_1 x_3 - \frac{R}{L_q} x_2 - P\frac{\Phi}{L_q} x_3 \\ P\frac{3}{2}\frac{\Phi}{J} x_2 - \frac{F}{J} x_3 - \frac{T_L}{J} \end{pmatrix} \tag{5}$$

The variables and parameters used in these equations are defined as follows :

- v_d, v_q : stator voltages in the direct and quadrature axes
- i_d, L_q : current and inductance in the direct axis
- i_q, L_q : current and inductance in the quadrature axis
- R : stator resistance
- Ω : mechanical speed of motor
- P : number of pole pairs
- Φ : flux linkage created by the rotor magnets
- J : moment of inertia
- F : viscous friction coefficient
- T_L : load torque
- f_1, f_2, f_3 : nonlinear terms in a PMSM model.

2. Nonlinear Speed Control of PMSM

In order to get a total input-output linearization, the direct axis current and mechanical speed are chosen as outputs. From eq.(1) and the assumption that the load torque is considered to be an unknown constant, differentiation of the output is taken until the direct relationship between the outputs and inputs of the model can be obtained as follows [7-9] :

$$\begin{pmatrix} \frac{di_d}{dt} \\ \frac{d^2\Omega}{dt^2} \end{pmatrix} = B + A \begin{pmatrix} v_d \\ v_q \end{pmatrix} \tag{6}$$

where

$$B = \begin{pmatrix} f_1 \\ \frac{3}{2}\frac{1}{J}\left\{P\Phi f_2 - \frac{2}{3}Ff_3\right\} \end{pmatrix} \tag{7}$$

$$A = \begin{pmatrix} \frac{1}{L_d} & 0 \\ 0 & \frac{3P\Phi}{2L_qJ} \end{pmatrix} \tag{8}$$

Because the order of eq.(1) is same as that of eq.(6), there is no internal dynamics. The nonlinear control input which permits a linearized and decoupled behavior is deduced from this relationship as follows :

$$\begin{pmatrix} v_d \\ v_q \end{pmatrix} = A^{-1}\left(-B + \begin{pmatrix} \nu_1 \\ \nu_2 \end{pmatrix}\right) \tag{9}$$

where ν_1 and ν_2 are the new control inputs. By Substituting eq.(9) into (6), the linearized and decoupled model can be given as

$$\frac{di_d}{dt} = \nu_1 \tag{10}$$

$$\frac{d^2\Omega}{dt^2} = \nu_2 \tag{11}$$

As the control laws for the new control inputs, the linear controller suggested by Le Pioufle becomes as follows [7] :

$$\nu_1 = K_{11}(i_d^* - i_d) \tag{12}$$

$$\nu_2 = \frac{d^2\Omega^*}{dt^2} + K_{21}\frac{d}{dt}(\Omega^* - \Omega) + K_{22}(\Omega^* - \Omega) \tag{13}$$

where K_{11}, K_{21}, and K_{22} are the gains. Also, i_d^* and Ω^* are the tracking commands of the direct axis current and mechanical speed of a PMSM, respectively. As a result, the following error dynamics can be obtained as

$$\frac{de_1}{dt} + K_{11}e_1 = 0 \tag{14}$$

$$\frac{d^2e_2}{dt^2} + K_{21}\frac{de_2}{dt} + K_{22}e_2 = 0 \tag{15}$$

where $e_1 = i_d^* - i_d$, $e_2 = \Omega^* - \Omega$. The poles for the desired error dynamics can be chosen by properly selecting the gains using a binomial standard form, etc. [10]. The overall scheme of the conventional nonlinear speed control system is shown in Fig. 1. As shown in this figure, by employing a rectilinear asymptotic speed trajectory generator, the acceleration command is within the maximum permissible value of a motor. As a result, the quadrature axis current can be made not exceed its maximum permissible value [7].

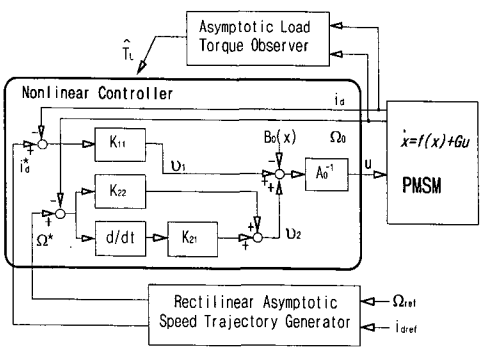

Fig. 1. Block diagram of the conventional nonlinear control scheme

3. Asymptotic Load Torque Observer

For the control scheme employed in this paper, the information on the acceleration is needed for state feedback and can be calculated from eq.(1). It is, however, required to estimate an unknown load torque. In a real system, there are many cases where some of the inputs are unknown or inaccessible. For the unknown and inaccessible inputs, the observer was studied by Meditch and Hostetter and a 0-observer is selected for simplicity [11]. The inaccessible load torque(T_L) can be assumed to be a slowly varying quantity compared with system dynamics. Thus, it is assumed to be an unknown constant. For a PMSM, the system equation for a disturbance torque observer can be expressed as follows :

$$\frac{dz}{dt} = Dz + Ew,\ y = \Omega = Cz \tag{16}$$

where

$$z = \begin{pmatrix} \Omega \\ T_L \end{pmatrix} = \begin{pmatrix} z_1 \\ z_2 \end{pmatrix}, D = \begin{pmatrix} \frac{-F}{J} & \frac{-1}{J} \\ 0 & 0 \end{pmatrix},$$

$$E = \begin{pmatrix} \frac{3P\Phi}{2J} \\ 0 \end{pmatrix}, C = (1\ 0), w = i_q$$

For this system, (D, C) is observable. The well-known asymptotic load torque observer can be designed as

$$\frac{d\hat{z}}{dt} = D\hat{z} + Ew + L(y - C\hat{z}) \tag{17}$$

where $\hat{z}$ is the observed value and $L = (l_1\ \ l_2)^T$ is the observer gain matrix.

III. Quasi-Linearized and Decoupled Model and Proposed Control Strategy

1. MRAS-based Estimation of Slowly Varying Parameters

To estimate the slowly varying parameters such as the resistance and flux, the concept of model reference adaptive system(MRAS) is employed. The dynamic equation of a real quadrature axis current of a PMSM is considered as a reference model. In a similar way, the dynamic equation of an observed quadrature axis current is considered as an adjustable model. The difference between the reference model and adjustable model can be reduced by an adaptation mechanism [12-13].

From eq.(1), the reference model becomes

$$\frac{di_q}{dt} = -\frac{R}{L_q}i_q - P\frac{\Phi}{L_q}\Omega - P\frac{L_d}{L_q}i_d\Omega + \frac{v_q}{L_q} \tag{18}$$

Similarly, the adjustable model can be expressed as

$$\frac{d\hat{i}_q}{dt} = -\frac{\hat{R}}{L_q}\hat{i}_q - P\frac{\hat{\Phi}}{L_q}\Omega - P\frac{L_d}{L_q}i_d\Omega + \frac{v_q}{L_q} \tag{19}$$

where $\hat{R}$ and $\hat{\Phi}$ are the estimated parameters and $\hat{i}_q$ is the observed quadrature axis current.

To derive the parameter adaptation mechanisms, the Lyapunov stability theory is utilized. Let's define the error as $e = i_q - \hat{i}_q$. Then, from eqs. 18 and 19, the following equation can be obtained as

$$\frac{de}{dt} = -\frac{R}{L_q}e - \frac{(R-\hat{R})}{L_q}\hat{i}_q - P\frac{(\Phi-\hat{\Phi})}{L_q}\Omega$$

$$= -\frac{R}{L_q}e - \frac{\Delta R}{L_q}\hat{i}_q - P\frac{\Delta\Phi}{L_q}\Omega \tag{20}$$

Now, let V be a Lyapunov function candidate defined as follows :

$$V(e,\ \hat{R},\ \hat{\Phi}) = \frac{1}{2}\left[e^2 - \frac{1}{\gamma_1}\frac{(R-\hat{R})^2}{L_q} - \frac{1}{\gamma_2}\frac{(\Phi-\hat{\Phi})^2}{L_q}\right] \quad (21)$$

where γ_1 and γ_2 are the adaptation gains which are strictly positive real.

Then, the time derivative of V becomes

$$\frac{dV}{dt} = -\frac{R}{L_q}e^2 - \frac{1}{\gamma_1}\frac{(R-\hat{R})}{L_q}\left(\gamma_1 \hat{i}_q e + \frac{d\hat{R}}{dt}\right) - \frac{1}{\gamma_2}\frac{(\Phi-\hat{\Phi})}{L_q}\left(\gamma_2 P\Omega e + \frac{d\hat{\Phi}}{dt}\right) \quad (22)$$

From eq.(22), the adaptation mechanisms can be obtained by equating the second and third terms of the right hand side to zeroes as

$$\frac{d\hat{R}}{dt} = -\gamma_1 \hat{i}_q e, \quad \frac{d\hat{\Phi}}{dt} = -\gamma_2 P\Omega e \quad (23)$$

During the operation, the real quadrature axis current is continuously compared with the observed quadrature axis current. The error is used in adaptation mechanisms which adjust the parameters used for the feedback linearization as shown in Fig. 2.

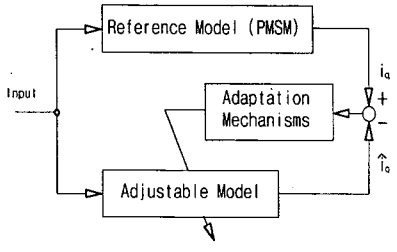

Fig. 2. Block diagram of MRAS-based parameter estimation scheme

2. *Effects of Parameter Estimation Errors*

From eqs.(22) and (23), the time derivative of the Lyapuov function candidate V can be written as

$$\frac{dV}{dt} = -\frac{R}{L_q}e^2 \le 0 \quad (24)$$

Since the time derivative of V is negative semidefinite, it follows that e, ΔR, and $\Delta\Phi$ are bounded. In steady state, the relationship between parameter estimation errors can be given as

$$\Delta R\ \hat{i}_q + \Delta\Phi\ P\Omega = 0 \quad (25)$$

This implies that ΔR and $\Delta\Phi$ are not linearly independent and do not necessarily converge to zero. The steady state estimation errors of these parameters are of opposite sign. Fig. 3 shows the typical effects of $\Delta\Phi$ and corresponding ΔR on the steady state speed error when the speed command is 1000 RPM. As shown in this figure, the effects of ΔR and $\Delta\Phi$ are canceled each other. Therefore, it can be concluded that the effects of the variations of the slowly varying parameters are effectively compensated even though there are some small estimation errors.

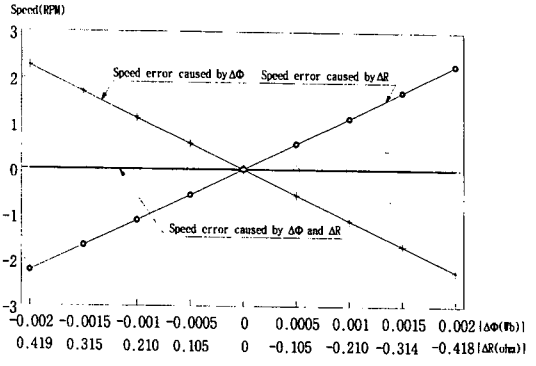

Fig. 3. Steady state speed error caused by estimation errors of flux and corresponding resistance

3. *Quasi-Linearized and Decoupled Model*

For the quickly varying parameter and disturbances, the actual nonlinear control input which employs the nominal parameter values and mechanical speed measured by a speed sensor can be expressed as follows :

$$\begin{pmatrix} v_d \\ v_q \end{pmatrix} = A_o^{-1}\left(-B_o + \begin{pmatrix} \nu'_1 \\ \nu'_2 \end{pmatrix}\right) \quad (26)$$

where ν'_1 and ν'_2 are the new control inputs and A_o, B_o are obtained from eqs.(7) and (8) using the nominal parameter values and measured speed. By Substituting eq.(26) into (6), a quasi-linearized and decoupled model can be obtained as follows :

$$\frac{di_d}{dt} = -P\frac{L_q}{L_d}i_q(\Omega_o - \Omega) + \nu'_1 = f_{n1}(x) + \nu'_1 \quad (27)$$

$$\frac{d^2\Omega}{dt^2} = -\frac{F}{J}(f_3 - f_{3o}) + P\frac{3\Phi}{2J}\left[\frac{P}{L_q}\Phi(\Omega_o - \Omega) + P\frac{L_d}{L_q}i_d(\Omega_o - \Omega)\right] + \frac{J_o}{J}\nu'_2 = f_{n2}(x) + b\nu'_2 \quad (28)$$

where the subscript "o" denotes the nominal parameter values and measured mechanical speed of motor. Unlike the linearized and decoupled model of eqs.(10) and (11), there are unwanted nonlinear terms $\hat{f}_{n2}(x)$ and $\hat{f}_{n1}(x)$, and control input gain b for the quasi-linearized and decoupled model of eqs.(19) and (20), which can degrade the control performances.

The unwanted nonlinear terms $f_{n1}(x)$ and $f_{n2}(x)$ are not exactly known but can be estimated as $\hat{f}_{n2}(x)$ and $\hat{f}_{n1}(x)$ and the estimation errors are bounded by some known functions $F_{n1}(x)$ and $F_{n2}(x)$. The control input gain b is also

unknown but its bound can be deduced. Now, we consider the feedback linearization technique as a model-simplifying device for the robust control [9], and the new control inputs ν'_1 and ν'_2 are derived using a boundary layer integral sliding mode control technique to overcome the drawbacks of the conventional nonlinear control scheme.

4. Control Strategy for the Quasi-Linearized and Decoupled Model

Assume the bounds of parameter variations and speed measurement error as follows :

$$J=\beta J_o,\ \beta_{\min}(=1.)\le\beta\le\beta_{\max}(=4.)$$
$$\Omega=\delta\Omega_o,\ \delta_{\min}(=0.95)\le\delta\le\delta_{\max}(=1.05) \quad (29)$$

Using eq.(29), the estimates $\hat{f}_{n1}(x)$ and $\hat{f}_{n2}(x)$, and the estimation error bounds $F_{n1}(x)$, $F_{n1}(x)$ of $f_{n1}(x)$, $f_{n2}(x)$ for the quasi-linearized and decoupled model can be obtained as follows :

$$\hat{f}_{n1}=-P\frac{L_q}{2L_d}i_q(2-\delta_{\min}-\delta_{\max})\Omega_o \quad (30)$$

$$F_{n1}=\left|P\frac{L_q}{2L_d}i_q(\delta_{\max}-\delta_{\min})\Omega_o\right| \quad (31)$$

$$\hat{f}_{n2}=\frac{1}{2}[\frac{3}{2}PFi_q\frac{\Phi_o}{J_o^2}(\frac{2}{\beta_{\min}}-\frac{1}{\beta_{\min}^2}-\frac{1}{\beta_{\max}\beta_{\min}})+\frac{F^2\Omega_o}{J_o}(\frac{\delta_{\min}}{\beta_{\min}\beta_{\max}}-\frac{2}{\beta_{\min}}+\frac{\delta_{\max}}{\beta_{\min}^2})+\frac{F\hat{T}_L}{J_o^2}(\frac{1}{\beta_{\min}\beta_{\max}}-\frac{2}{\beta_{\min}}+\frac{1}{\beta_{\min}^2})]+\frac{1}{2}[P\frac{3\hat{\Phi}}{2J_o}[\frac{1}{\beta_{\min}}P\frac{L_d}{L_q}(1-\delta_{\max})\Omega_o i_d+\frac{1}{\beta_{\min}}P\frac{(1-\delta_{\max})}{L_q}\hat{\Phi}\Omega_o+\frac{1}{\beta_{\min}}P\frac{L_d}{L_q}(1-\delta_{\min})\Omega_o i_d+\frac{1}{\beta_{\min}}P\frac{(1-\delta_{\min})}{L_q}\hat{\Phi}\Omega_o]] \quad (32)$$

$$F_{n2}=|\frac{1}{2}[\frac{3}{2}PFi_q\frac{\hat{\Phi}}{J_o^2}(\frac{1}{\beta_{\min}^2}-\frac{1}{\beta_{\max}\beta_{\min}})+\frac{F^2\Omega_o}{J_o}(-\frac{\delta_{\min}}{\beta_{\min}\beta_{\max}}+\frac{\delta_{\max}}{\beta_{\min}^2})+\frac{F\hat{T}_L}{J_o^2}(-\frac{1}{\beta_{\min}\beta_{\max}}+\frac{1}{\beta_{\min}^2})]+\frac{1}{2}[P\frac{3\hat{\Phi}}{2J_o}[-\frac{1}{\beta_{\min}}P\frac{L_d}{L_q}(1-\delta_{\max})\Omega_o i_d-\frac{1}{\beta_{\min}}P\frac{(1-\delta_{\max})}{L_q}\hat{\Phi}\Omega_o+\frac{1}{\beta_{\min}}P\frac{L_d}{L_q}(1-\delta_{\min})\Omega_o i_d+\frac{1}{\beta_{\min}}P\frac{(1-\delta_{\min})}{L_q}\hat{\Phi}\Omega_o]]| \quad (33)$$

The bound on control input gain is

$$b_{\min}(=\frac{1}{\beta_{\max}}=0.25)\le b\le b_{\max}(=\frac{1}{\beta_{\min}}=1.0) \quad (34)$$

Using eqs.(30) through (34), the design problem of the sliding mode controller for the quasi-linearized and decoupled model of eqs.(27) and (28) is well introduced in a previous work [9]. The boundary layer integral sliding mode controller is considered to avoid the chattering phenomenon and the reaching phase problem [9, 12-13]. The sliding surface s_1 is chosen for the input-output decoupled form of eq.(27) [9, 16].

$$s_1=(\frac{d}{dt}+\lambda_1)\int_0^t e_1dt=e_1+\lambda_1\int_0^t e_1dt-e_1(0) \quad (35)$$

And the control law for ν'_1 is designed to guarantee $s_1\dot{s}_1<-\eta_1|s_1|$ as

$$\nu'_1=\hat{\nu}_1-k_1 sat(\frac{s_1}{\phi_1}) \quad (36)$$

where $\hat{\nu}_1=-\hat{f}_{n1}-\lambda_1 e_1$, $k_1=F_{n1}+\eta_1$, and $sat(\cdot)$ is the saturation function. Also, λ_1 and η_1 are the strictly positive constants. From eq.(35), it can be noted that $s_1=0$ from time $t=0$ and there is no reaching phase problem.

From the bound on control input gain b of eq.(34), the geometric mean b_m can be defined as

$$b_m=(b_{\min}b_{\max})^{1/2}=(\frac{1}{\beta_{\max}\beta_{\min}})^{1/2} \quad (37)$$

The bound on b can then be written in the form of

$$\Psi^{-1}\le\frac{b_m}{b}\le\Psi \quad (38)$$

where

$$\Psi=(\frac{b_{\max}}{b_{\min}})^{1/2}=(\frac{\beta_{\max}}{\beta_{\min}})^{1/2}$$

The sliding surface s_2 is chosen for the input-output decoupled form of eq.(28) [9, 16].

$$s_2=\left(\frac{d}{dt}+\lambda_2\right)^2\int_0^t e_2\,dt=\frac{de_2}{dt}+2\lambda_2 e_2+\lambda_2^2\int_0^t e_2\,dt-\frac{de_2}{dt}|_{t=0}-2\lambda_2 e_2(0) \quad (39)$$

The control law for ν'_2 is designed as shown in eq.(40) to guarantee $s_2\dot{s}_2<-\eta_2|s_2|$.

$$\nu'_2=b_m^{-1}(\hat{\nu}_2-k_2 sat(\frac{s_2}{\phi_2})) \quad (40)$$

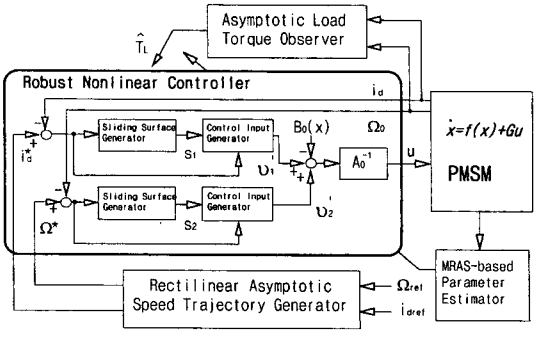

Fig. 4. Block diagram of the proposed robust nonlinear control scheme

where $\hat{\nu}_2 = -\hat{f}_{n2} - 2\lambda_2 de_2/dt - \lambda_2^2 e_2$, $k_2 = \Psi(F_{n2} + \eta_2) + (\Psi - 1)|\hat{\nu}_2|$, and λ_2 and η_2 are strictly positive constants. From eq.(39), it can also be noted that $s_2 = 0$ from time $t = 0$ and there is no reaching phase problem.

The bounds of uncertainties of the unwanted terms needed for the robust nonlinear control are obtained by deriving a quasi-linearized and decoupled model and the robustness is obtained by using these bounds to generate the control inputs which compensate the parameter uncertainties and speed measurement error. The overall scheme of the proposed robust nonlinear speed control system is shown in Fig. 4.

IV. Simulations and Experimental Results

1. System Configuration

The simulations and experimental works are carried out for the PMSM with the specifications as listed below.

$R_o = 3\ ohm,\ L_d = L_q = 7\ mH,\ \Phi_o = 0.167\ Wb,$

$J_o = 1.314 \cdot 10^{-4} Nmsec^2,\ F = 2 \cdot 10^{-3} Nmsec,\ P = 2$

rated speed $= 3000$ *RPM, rated power* $= 400$ *W, rated torque* $= 1.274$ *Nm* .

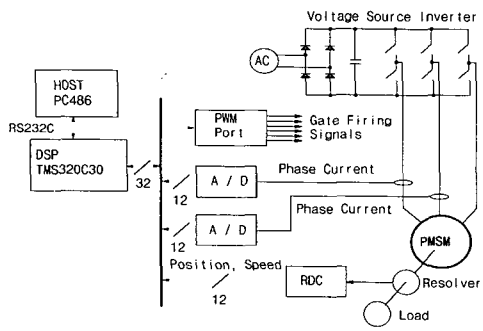

Fig. 5. Configuration of DSP-based experimental system

The configuration of the DSP-based experimental system is shown in Fig. 5. The main processor of the experimental system is a floating point Digital Signal Processor TMS320C30 with clock frequency of 32MHz [17-18]. The PMSM is driven by a three phase voltage source PWM inverter using an intelligent power module with a switching frequency of 7.8 kHz. The brushless resolver and resolver to digital converter are used to detect the absolute rotor position and speed of the PMSM. The resolution of detected position is selected as 12 bits. The phase currents are detected by the Hall-effect devices and the measured analogue signals are converted to digital values using the Analog to Digital converter with a 12 bit resolution. The PWM gate firing signals for the desired phase voltage commands are generated by using the space vector modulation technique [19]. The sampling period of the control system is set as 128 μsec.

To examine the performance of the proposed control scheme, the dynamic behavior of the control system is tested under the inertia or flux variations in the acceleration region with the acceleration time of 50 msec.

2. Simulation Results

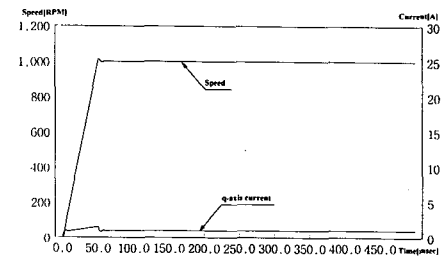

(a) Conventional control scheme

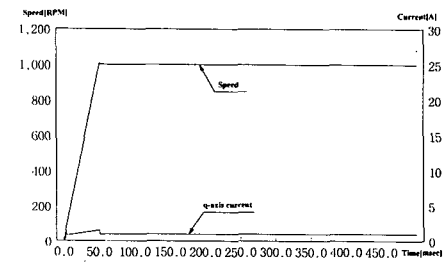

(b) Proposed control scheme

Fig. 6. Speed response and q-axis current under no inertia variation

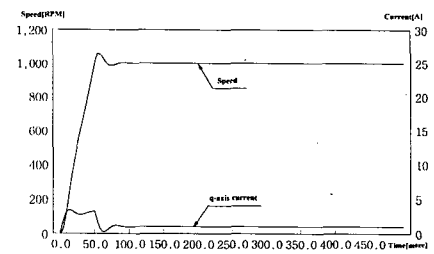

(a) Conventional control scheme

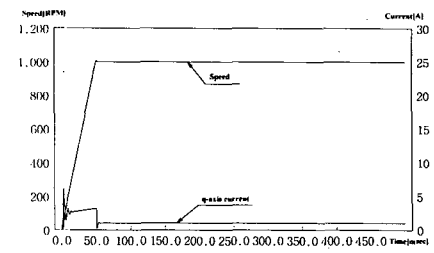

(b) Proposed control scheme

Fig. 7. Speed response and q-axis current under inertia variation($J = 4J_o$)

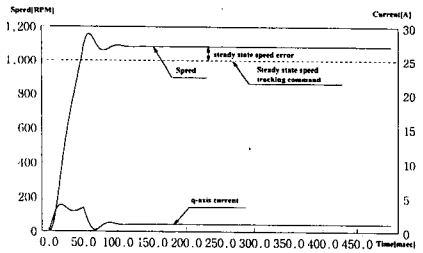

(a) Conventional control scheme

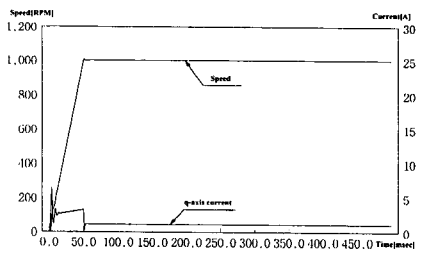

(b) Proposed control scheme

Fig. 8. Speed response and q-axis current under inertia variation($J=4J_o$) and +30% flux variation

To show the validity of the proposed control scheme, the computer simulations are carried out for the systems shown in Figs. 1 and 4 under various conditions. Fig. 1 shows the overall block diagram of the conventional nonlinear speed controller and Fig. 4 shows the proposed robust nonlinear speed controller. The design parameters ($K_{11}=2100$, $K_{21}=700$, and $K_{22}=490000$) used for the conventional nonlinear control scheme are selected to obtain nearly the same performances as those of the proposed control scheme when there are no parameter variations or disturbances. For the proposed robust nonlinear control scheme, the design parameters are selected as $\gamma_1=\gamma_2=0.5$, $\lambda_1=2100$, $\lambda_2=700$, $\eta_1=1$, $\eta_2=10$, $\phi_1=0.005$, and $\phi_2=5000$. It can be noted from eq.(39) that the sliding surface is a weighted sum of terms related to a tracking error and the large boundary layer thickness does not mean a large tracking error [9]. The observer gains used for the asymptotic load torque observer are selected as $l_1=796.67$ and $l_2=-21.024$ to locate the double observer poles at -400 when there are no parameter variations. Figs. 6(a) and (b) show the speed response and quadrature axis current under no inertia variation($J=J_o$) for both control schemes. Figs. 7(a) and (b) show the same phenomena under the inertia variation of 4 times the nominal value($J=4J_o$). As shown in Figs. 6(a) and 7(a), the conventional nonlinear control scheme shows significant degradation in the transient response. Under the inertia variation of 4 times the nominal value, it shows the enhanced overshoot of 5.5% and prolonged settling time of 75msec. However, as shown in Figs. 6(b) and 7(b), the proposed robust nonlinear control scheme shows a good performance without such a degradation. Fig. 8 shows the case of inertia variation of 4 times the nominal value and +30% flux variation. As shown in this figure, the conventional scheme shows the enhanced overshoot of 16% and steady state speed error. It can be noted from this figure that the additional degradation in the transient and steady state responses are occurred due to flux uncertainties. However, the proposed robust nonlinear control scheme shows a good performance without such degradations.

3. *Experimental Results*

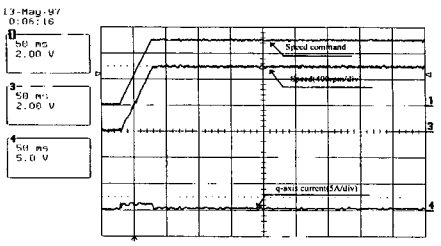

(a) Conventional control scheme

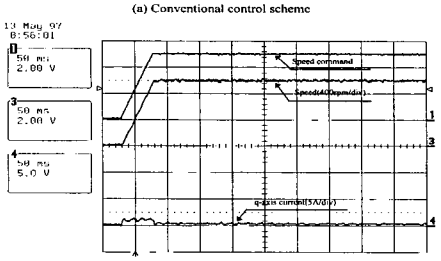

(b) Proposed control scheme

Fig. 9. Speed response and q-axis current under no inertia variation [experiments]

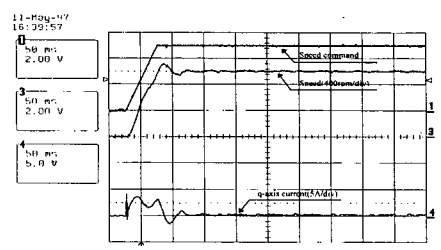

(a) Conventional control scheme

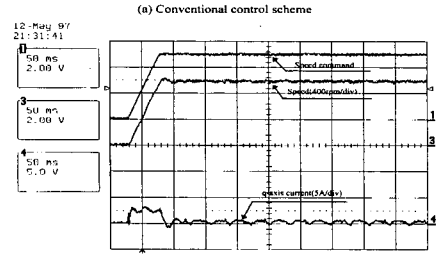

(b) Proposed control scheme

Fig. 10. Speed response and q-axis current under inertia variation($J=4J_o$) [experiments]

The experimental works are carried out for the conventional and proposed control schemes. The same design parameters given in the previous section are used in both

control schemes. The dynamic responses for both control schemes under the various conditions are shown in Figs. 9-14. As shown in Figs. 9(a) and (b), both control schemes provide good dynamic responses corresponding to the design specifications when there is no inertia variation($J=J_o$). However, when the inertial load is increased($J=4J_o$) in the conventional nonlinear control scheme, the overshoot and settling time are increased up to 6% and 70 msec as shown in Fig. 10(a). On the other hand, the proposed improved nonlinear control scheme provides the nearly same responses for both cases as shown in Figs. 9(b) and 10(b). For the case of inertia variation of 4 times the nominal value and +30% flux variation, the conventional control scheme shows the increased overshoot of 16% and steady state speed error as shown in Fig. 11(a). However, the proposed control scheme provides a good response as shown in Fig. 11(b). It can be observed from the experimental results in Figs. 9(b), 10(b) and 11(b) that there are no control chattering in the quadrature axis current by employing the boundary layers [9]. Even though some differences exist between simulations and experimental results mainly due to the unknown friction coefficient, and so on, it can be considered that the above simulations and experimental results well verify the validity of the proposed robust nonlinear control scheme.

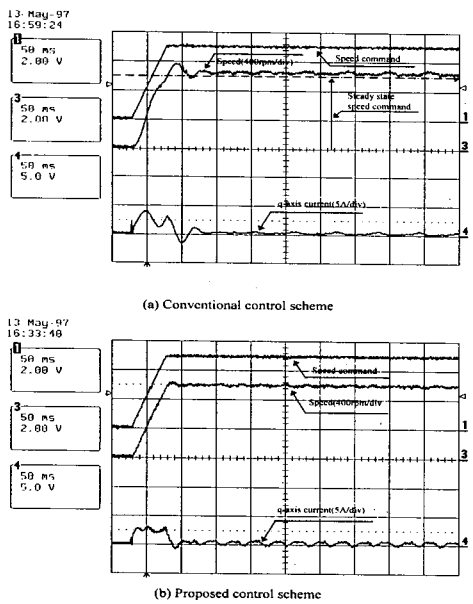

Fig. 11. Speed response and q-axis current under inertia variation($J=4J_o$) and +30% flux variation [experiments]

Fig. 12 shows the estimated flux for the proposed control scheme when there is +30% flux variations. As shown in this figure, it can be said that the parameter estimation scheme shows a reasonable performance. Fig. 13 shows the values of sliding surfaces s_1 and s_2 during speed transient for the proposed control scheme when there are inertia variation of 4 times the nominal value and +30% flux variation. It can be noted that the sliding surfaces are bounded within the boundary layers and these values are zeroes at the beginning of control actions. Therefore, it can be said that the sliding conditions are satisfied from the beginning of control actions without reaching phase problems. The values of sliding surfaces s_1 and s_2 at steady state are shown in Fig. 14 when there are inertia variation of 4 times the nominal value and +30% flux variation. It can be noted that the value of sliding surface s_2 is decreased to a small value within the boundary layer at steady state.

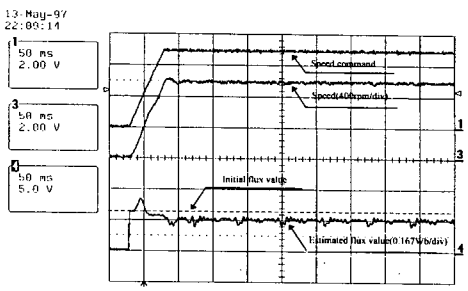

Fig. 12. Values of estimated flux under +30% flux variation [experiment]

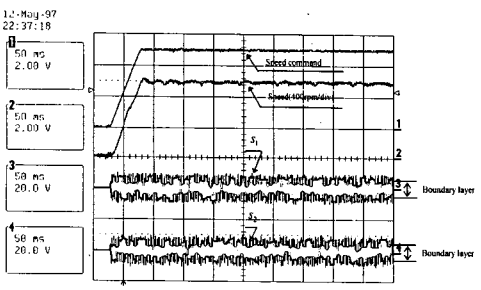

Fig. 13. Values of sliding surfaces s_1 and s_2 during speed transient under inertia variation($J=4J_o$) and +30% flux variation [experiment]

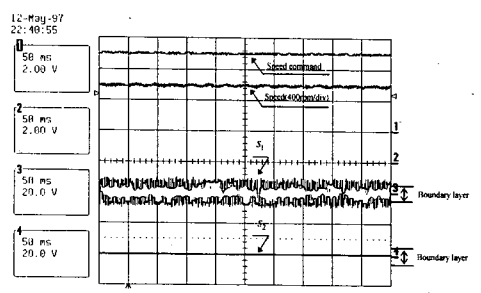

Fig. 14. Values of sliding surfaces s_1 and s_2 under inertia variation($J=4J_o$) and +30% flux variation at steady state [experiment]

V. Conclusion

This paper proposes a robust nonlinear speed control scheme for a PMSM which guarantees the robustness in the presence of parameter variations and speed measurement error. The MRAS-based adaptation mechanisms for the estimation of slowly varying parameters are derived using the Lyapunov stability theory. For the quickly varying parameters and disturbances, the influence of parameter variations and speed measurement error on the nonlinear speed control of a PMSM is investigated and a quasi-linearized and decoupled model is derived. Based on this model, the design methods for the proposed control scheme have been given using the boundary layer integral sliding mode control technique. The bounds of uncertainties needed for the sliding mode control are deduced and the robustness is obtained by using these bounds to generate the control inputs which compensate the parameter uncertainties and disturbances. By introducing the boundary layer integral sliding mode technique, the chattering phenomenon and reaching phase problem can be avoided.
To show the validity of the proposed control scheme, the comparative simulations and experiments were carried out under various conditions. The distinctive results of this study can be summarized as follows. Compared with the conventional nonlinear control scheme, the proposed robust nonlinear control scheme provides good transient and steady state performances under the inertia and flux variations. For the proposed control scheme, the MRAS-based adaptation mechanisms for the estimation of slowly varying parameters show reasonable performances. Also, the chattering phenomenon and reaching phase problem can be avoided by introducing boundary layer integral sliding mode technique. It can be said from these results that the proposed control scheme has the robustness against the unknown disturbances. Therefore, it can be expected that the proposed control scheme can be applied to the high performance applications such as the machine tools and robots.

References

[1] G. Champenois, P. Mollard, and J. P. Rognon, "Synchronous servo drive: a special application", *IEEE-IAS Conf. Rec.*, 1986, pp. 182-189.

[2] M. Fadel and B. De Fornel, "Control laws of a synchronous machine fed by a PWM voltage source inverter", *EPE*, Aachen, RFA, Oct. 1989.

[3] W. Leonhard, *Control of electrical drives.* Springer Verlag,1985.

[4] T. Rekioua, F. Meibody Tabar, J. P. Caron, and R. Le Doeuff, "Study and comparison of two different methods of current control of a permanent magnet synchronous motor", *Conf. Rec. IMACS-TC1*, Nancy, France, Vol.1, pp. 157-163, 1990.

[5] B. Le Pioufle and J. P. Louis, "Influence of the dynamics of the mechanical speed of a synchronous servomotor on its torque regulation, proposal of a robust solution", *EPE*, Florence, Vol. 3, pp. 412-417, 1991.

[6] J. J. Carroll Jr. and D. M. Dawson, "Integrator backstepping techniques for the tracking control of permanent magnet brush DC motors", *IEEE Trans. IA*, Vol. 31, no. 2, pp. 248-255, Mar./April 1995.

[7] B. Le Pioufle, "Comparison of speed nonlinear control strategies for the synchronous servomotor", *Electric Machines and Power Systems*, Vol.21, pp. 151-169, 1993.

[8] A. Isidori, *Nonlinear control systems: an introduction.* Springer-Verlag, 1985.

[9] J. J. Slotine and W. Li, *Applied nonlinear control.* Prentice-Hall, 1991.

[10] I. J. Nagrath and M. Gopal, *Control systems engineering.* John Wiley & Sons, 1982.

[11] J. Meditch and G. Hostetter, "Observers for systems with unknown and inaccessible inputs", *Int. J. Control*, Vol.19, no. 3, pp. 473-480, 1974.

[12] K. S. Narendra and A. M. Annaswamy, *Stable adaptive systems.* Prentice-Hall, 1989.

[13] K. J. Astrom and B. Wittenmark, *Adaptive control.* Addison Wesley, 1995.

[14] T. L. Chern and Y. C. Wu, "Design of brushless DC position servo systems using integral variable structure approach", *IEE Proc.-B Electric Power Applications*, Vol.140, no.1, pp. 27-34, 1993.

[15] J. H. Lee, J. S. Ko, S. K. Chung, D. S. Lee, J. J. Lee, and M. J. Youn, "Continuous variable structure controller for BLDDM with prescrived tracking performance", *IEEE Trans. IE*, Vol.41, no.5, pp. 483-491, 1994.

[16] J. Y. Hung, W. Gao, and J. C. Hung, "Variable structure control: A survey", *IEEE Trans. IE*, Vol.40, no.1, pp. 2-22, 1993.

[17] TMS320C3X Users Guide, Texas Instruments Inc., 1990.

[18] TMS320C30 Assembly Language Tools Users Guide, Texas Instruments Inc., 1990.

[19] T. Kenjo, *Power Electronics for the Microprocessor Age.* Oxford University Press, 1990.

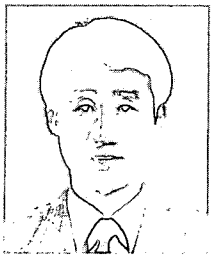

In-Cheol Baik was born in Seoul, Korea on February 25, 1962. He received the B.S. degree in electronics from Konkuk University in 1984 and the M.S. and Ph.D. degrees in electrical engineering from the Korea Advanced Institute of Science and Technology (KAIST) in 1987 and 1998. respectively. He was a recipient of the University scholarship from Konkuk University during 1980~1982. He has been with the Living system research laboratory of LG Electronics Inc., Seoul from 1987. From February to May 1990, he took the Application Engineer course at SIEMENS Energy & Automation Training Center, Manchester, U.K. His research interests include rotating electrical machine drive systems, electric power conversion systems, and control engineering. Dr. Baik is a member of the Korean Institute of Power Electronics(KIPE) and KIEE.

Kwan-Yuhl Cho was born Chunra-Namdo, Korea on February 20, 1963. He received the B. S. degree from Seoul National University, Korea in 1986 and the M.S. and Ph.D. degrees in electrical engineering from the KAIST (Korea Advanced Institute of Science and Technology) in 1988 and 1993, respectively. He has been with LG Electronics since 1993. His research activities are in the areas on power electronics and control including the drive system, and the application of the motors and drives to the home appliances.

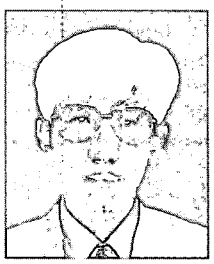

Kyeong-Hwa Kim was born in Seoul, Korea, on March 11, 1969. He received the B. S. degree in Electrical Engineering from Han-Yang University. Seoul, Korea, in 1991 and the M. S. degree in Electrical Engineering from Korea Advanced Institute of Science and Technology(KAIST), Taejon, Korea, in 1993. He is currently working toward the Ph. D. degree in Electrical Engineering at KAIST. His research interests are in the areas on power electronics and control, which include ac machine drives and microprocessor-based control applications.

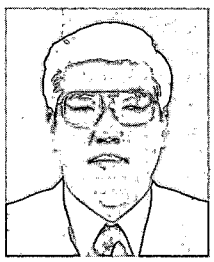

Myung-Joong Youn was born in Seoul, Korea on November 26, 1946. He received the B. S. Degree from Seoul National University, Seoul, Korea in 1970 and the M. S. and Ph.D. degrees in electrical engineering from the University of Missouri-Columbia in 1974 and 1978, respectively. He was with the Aircraft Equipment Division of General Electric Company at Erie, Pennsylvania, since 1978, where he was an Individual Contributor on Aerospace Electrical Engineering. He has been with the Korea Advanced Institute of Sciene and Technology since 1983 where he is now a professor. His research activities are in the areas on power electronics and control which include the drive system, rotating electrical machine design, and high performance switching regulators. Prof. Youn is a member of the KIPE, KIEE, and IEEK.